Brightness of Solar Magnetic Elements as a Function of Magnetic Flux at High Spatial Resolution

Fatima Kahil

S. Solanki & T. Riethmüller
Max Planck Institute for Solar System Research-Göttingen, Germany

September 9, 2016

Introduction - Magnetic elements

- Brightness of magnetic features in Plage and Network has been a subject of major studies
- Insights into radiative energy transport
- Enhanced brightness in both continuum and line core of spectral lines
- Contribution of magnetic elements to the TSI variations over the solar cycle: 30% at continumm wavelengths, and 60% at wavelengths below 400 nm (Krivova et al. 2006)
- Chromospheric structuring and heating of the outer atmosphere (Schrijver et al. 1989)

Brightness of magnetic elements vs. B_{LOS}

- Topka et al. (1992,1997); Title et al. (1992)
- Swedich Solar Observatory at 676.8, 557.6 and 630.2 nm
- Spatial resolution: 0.3″
- Contrast decreases with magnetic flux at disc centre for active regions

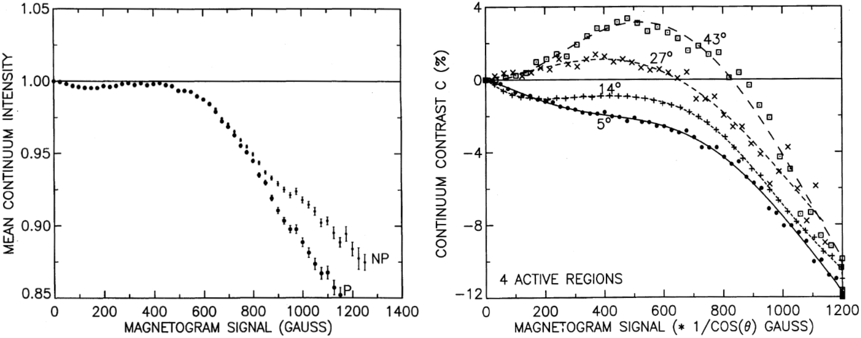

Figure : Title et al.(1992); Topka et al.(1992)

Brightness of magnetic elements vs. B_{LOS}

- Lawrence et al. (1993): QS network data/SSO
- Contrast is positive at intermediate field strengths, and increases for higher values

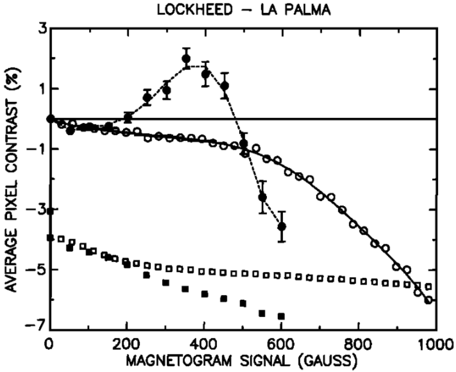

Figure : Lawrence et al.(1993), disc centre

Brightness of magnetic elements vs. B_{LOS}

- Kobel et al. (2011)
- Solar Optical Telescope/Hinode
- Resolution: 0.3″
- Fe I 630.15 and 630.25 nm
- Contrast peaks at ≈ 700 G for both regions

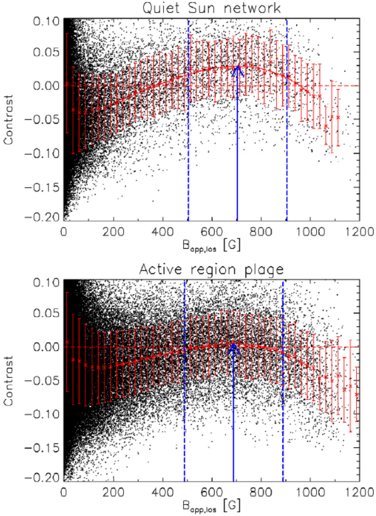

Brightness of magnetic elements vs. B_{LOS}

- Röhrbein et al. (2011)
- MURaM simulations (Vögler et al. 2005)
- Plage region (200 G)
- $\lambda = 630.2$ nm
- Convolution with D =1 m, 0.5 m Airy functions

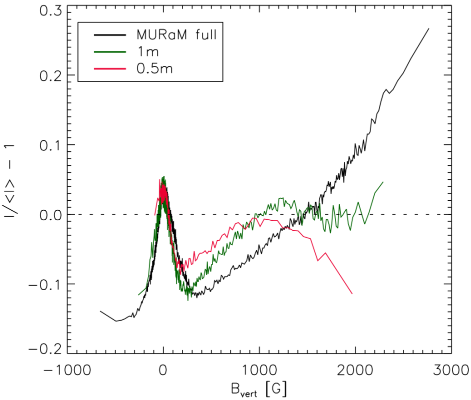

Aims & Motivation

- Sunrise: Balloon-borne solar observatory/1 m telescope/UV filter imager/imaging vector polarimeter (@ $\sim$ 37 km)
- Diffraction limited angular resolution: $0.05''$ (35 km) at 214 nm, and $0.1''$(70 km) in the visible
- High angular, temporal, and spectral resolution observations, in the visible and UV down to 200 nm

Aims & Motivation

- Sunrise: Balloon-borne solar observatory/1 m telescope/UV filter imager/imaging vector polarimeter (@ $\sim$ 37 km)
- Diffraction limited angular resolution: $0.05''$ (35 km) at 214 nm, and $0.1''$(70 km) in the visible
- High angular, temporal, and spectral resolution observations, in the visible and UV down to 200 nm

Aims

- Relationship between the brightness in the continuum and NUV, with B_{los}
- Relationship between the lower chromosphere emission and B_{los}
- Constrain radiative MHD simulations of flux tube models

IMaX and SuFI Data

Imaging Magnetograph eXperiment

- Time series 14:22 to 15:00 UT (40 quiet Sun magnetograms).
- Fe I (λ_0 =5250.2 Å) spectral line (g=3).
- Exposure time = 250 ms, cadence = 32 sec.
- $\Delta\lambda = \{-80, -40, +40, +80, +227\}$ mÅ.
- plate scale = 0.054458 arcsec/pixel (40 km/pixel).
- FOV = $50'' \times 50''$ (936×936 pixels).

Sunrise Filter Imager

λ(nm)	FWHM(nm)	Exp.time(sec)	plate scale(″/pixel)
214[1]	10	30	0.01983
300	5	0.3	0.0207
313(OH-band)	1.2	0.2	0.0203
388(CN-band)	0.8	0.1	0.01987
397(Ca II H-line core)[2]	0.18	1	0.01983

[1] middle/upper photosphere
[2] lower chromosphere

Data Preparation - Stokes inversions

- Stokes images corrected for 12% global stray light
- Spectral scans interpolated with respect to time
- Data PD reconstructed and de-jittered
- Inversion with SPINOR (The **S**tokes-**P**rofiles-**IN**version-**O**-**R**outines) code:
    - Three temperature nodes at $\log \tau =$ -2.5, -0.9, 0
    - Height independent B, V_{LOS}, micro-turbulence
    - Quantity of interest: $B_{\mathrm{LOS}} = |B| \times \cos \gamma$

- Sufi at 214 nm, 300 nm, 313 nm, and 388 mm with IMaX Stokes I continuum at 525.02 nm.
- Sufi at 397 nm (core of CaII H) with IMaX stokes I line core
- Resampling to the same pixel size (IMaX's 0.05"/pixel)
- Cross-Correlation technique to find IMaX-SuFI offsets to a sub-pixel accuracy $\Longrightarrow$ Common FOV off all images ($13'' \times 38''$)

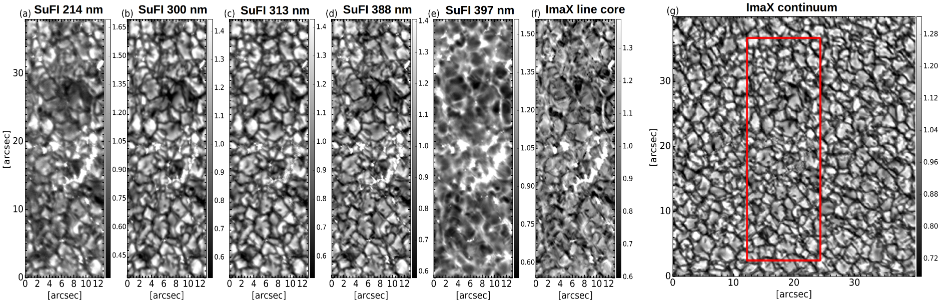

Data Analysis - Contrast

- Contrast at each pixel for each wavelegnth band $\mathrm{WB} = \{\mathrm{CONT}, \mathrm{LC}, 214, 300, 313, 388, 397\}$ is computed as follows:

$$C_{\mathrm{WB}} = \frac{I_{\mathrm{WB}}}{I_{\mathrm{WB,QS}}}$$

- C_{CONT}, C_{LC}:the IMaX Stokes I continuum and line-core (derived from Gaussian fits) intensity contrasts
- $I_{\mathrm{WB,QS}}$ is the mean quiet-Sun intensity averaged over the entire common FOV (CFOV)
  - SUFI+IMaX: CFOV is $13'' \times 38''$
  - IMaX intensity+B maps: $40'' \times 40''$

Results - Visible continuum contrast vs. B_{LOS}

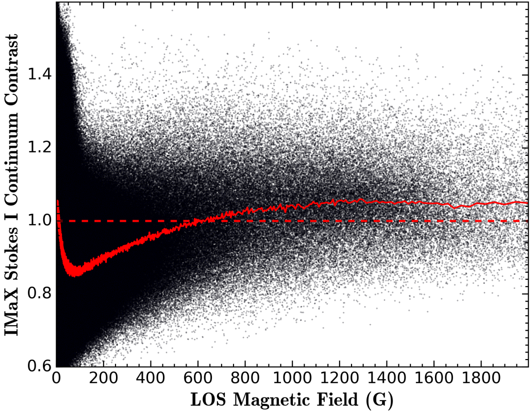

Figure : IMaX (0.15"/Fe I 525.04 nm), Kahil et al. (2016)

Results - Visible continuum contrast vs. B_{LOS}

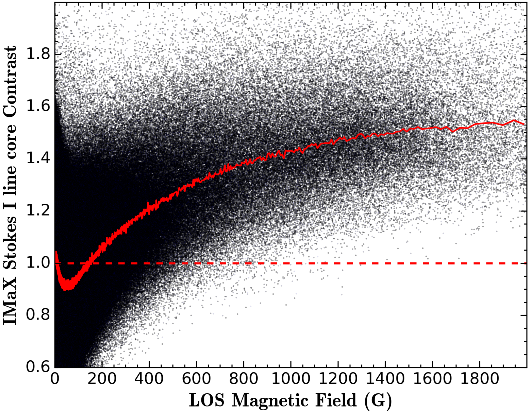

Figure : Line core contrast vs. B_{LOS}

Results - Visible continuum contrast vs. B_{LOS}

- Stokes I and V degraded to Hinode's spatial resolution
- Convolution with a Gaussian of FWHM $= 0.32''$
- Centre of gravity method (C-O-G) to derive B_{LOS}

Results - Visible continuum contrast vs. B_{LOS}

- Stokes I and V degraded to Hinode's spatial resolution
- Convolution with a Gaussian of FWHM $= 0.32''$
- Centre of gravity method (C-O-G) to derive $B_{\rm LOS}$

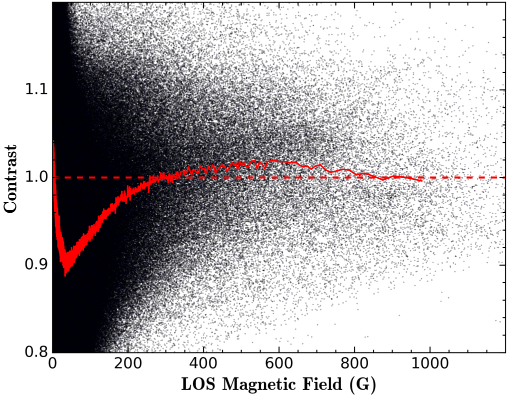

Results - Chromospheric emission vs. B_{LOS}

- QS is responsible for the heating of the outer chromosphere.
- Ca II-H line: chromospheric diagnostic

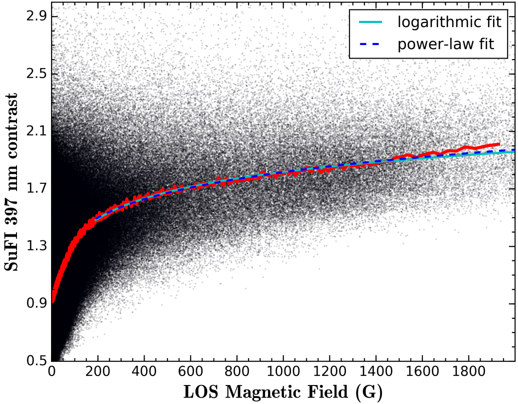

author	b	comments
Schrijver et al.(1989)	0.66	Mount Wislon (AR's)
Ortiz and Rast(2005)	0.6	SOHO/MDI (QS)
Rezai et al.(2007)	0.2	VTT (QS N+IN)
Loukitcheva et al.(2009)	0.31	BBSO+SOHO/MDI (time averaged data)

$$I = a.B_{\mathrm{LOS}}^b + I_0 \quad (1)$$

I_0: basal flux

$$I = a'.\log_{10}(B_{\mathrm{LOS}}) + b' \quad (2)$$

cut(G)	b	χ^2 (1)	χ^2 (2)
190	0.14±0.02	0.91	1.00
210	0.16±0.03	0.86	0.96
230	0.21±0.03	0.81	0.94
250	0.28±0.04	0.72	0.90

Results - UV brightness vs. B_{LOS}

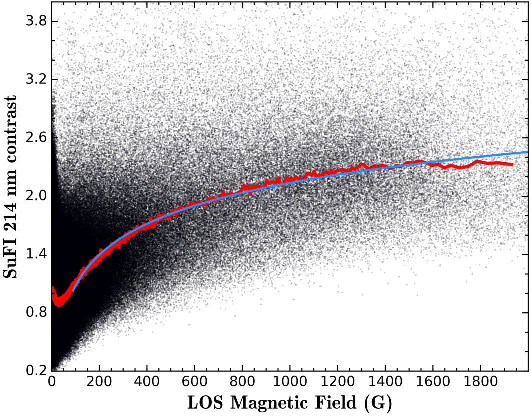

$$\frac{I}{<I_{qs}>} = a.\log_{10}(B_{\mathrm{LOS}}) + b$$

cut(G)	a	b	χ^2
90	1.06±0.004	-1.04±0.009	2.38
100	1.07±0.004	-1.07±0.01	1.94
150	1.10±0.005	-1.17±0.01	1.13
200	1.11±0.007	-1.2±0.02	0.93
250	1.11±0.009	-1.18±0.02	0.82

Results - UV brightness vs. B_{LOS}

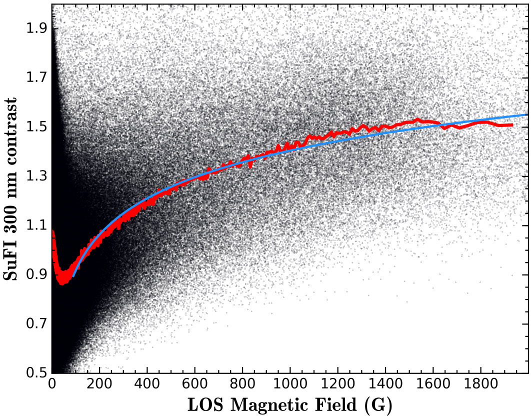

$$\frac{I}{<I_{qs}>} = a.\log_{10}(B_{\mathrm{LOS}}) + b$$

cut(G)	a	b	χ^2
90	0.48±0.002	-0.06±0.006	3.34
100	0.50±0.002	-0.08±0.006	2.82
150	0.52±0.002	-0.16±0.007	1.35
200	0.54±0.003	-0.20±0.008	0.91
250	0.54±0.004	-0.22±0.01	0.80

Results - UV brightness vs. B_{LOS}

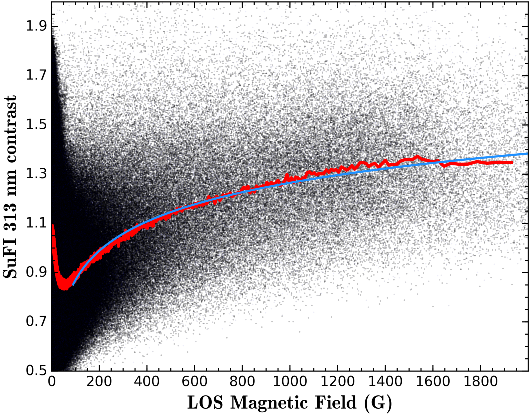

$$\frac{I}{<I_{qs}>} = a.\log_{10}(B_{\mathrm{LOS}}) + b$$

cut(G)	a	b	χ^2
90	0.39±0.002	0.08±0.004	2.84
100	0.40±0.002	0.06±0.005	2.25
150	0.42±0.002	0.06±0.005	1.11
200	0.43±0.002	-0.03±0.007	0.84
250	0.44±0.003	-0.04±0.009	0.72

Results - UV brightness vs. B_{LOS}

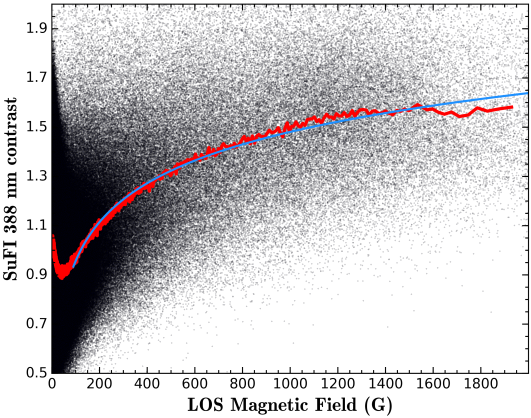

$$\frac{I}{<I_{qs}>} = a.\log_{10}(B_{\mathrm{LOS}}) + b$$

cut(G)	a	b	χ^2
90	0.52±0.002	-0.09±0.005	2.56
100	0.53±0.002	-0.11±0.005	2.10
150	0.54±0.003	-0.16±0.007	1.43
200	0.55±0.004	-0.17±0.01	1.24
250	0.55±0.005	-0.16±0.01	1.15

All wavelengths

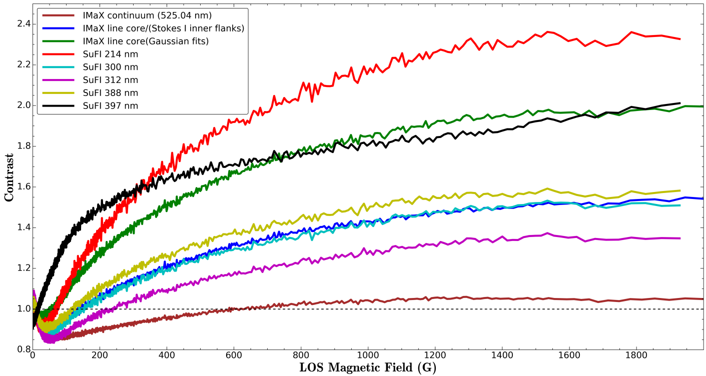

C-O-G vs. Inversions

- C-O-G applied on stray-light corrected stokes profiles (lev2.3) *Centre of gravity method* (Rees & Semel 1979):

$$\lambda_{\pm} = \frac{\int_{-\infty}^{+\infty} \Delta\lambda [I_c - (I \pm V)] d\Delta\lambda}{\int_{-\infty}^{+\infty} (I_c - (I \pm V)) d\Delta\lambda}$$

$$B_{LOS} = \frac{|\Delta\lambda_Z|}{C_0 \times g \times \lambda_0^2}, \quad \Delta\lambda_Z = \frac{\lambda_+ - \lambda_-}{2}$$

C-O-G vs. Inversions

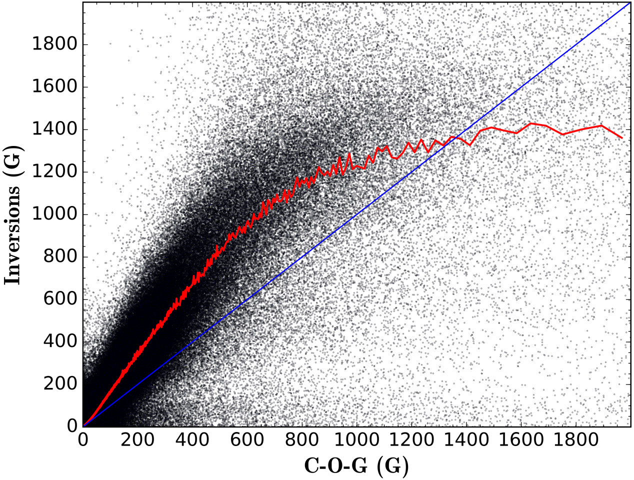

Figure : B_{los} derived from inversions vs. B_{los} from C-O-G on IMaX data points

C-O-G vs. Inversions

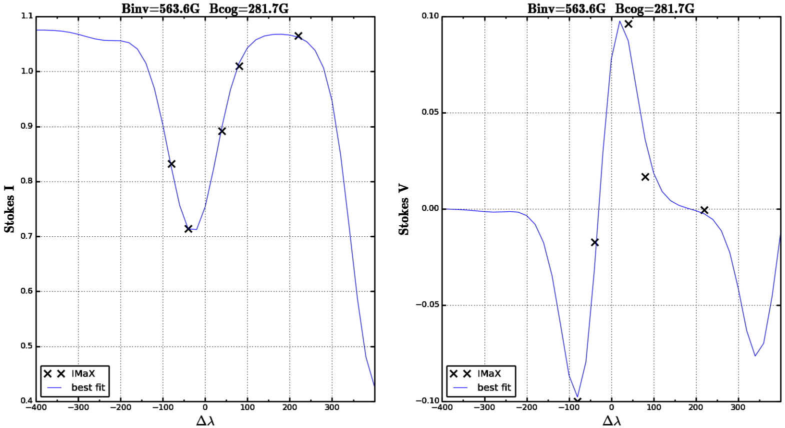

C-O-G vs. Inversions

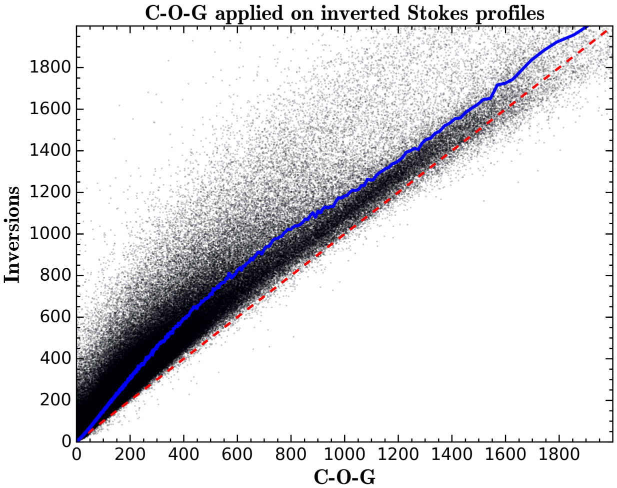

Figure : B_{los} derived from inversions vs. B_{los} from C-O-G on inverted profiles

Future projects

- Carry the same study for different heliocentric angles
- Extend the study to active region Plage (SUNRISE II)
- Compare MHD simulations with observational results to asses the effect of limited spatial resolution

Thank you for your attention!